

Influence of rhodium additive on hydrogen electrosorption in palladium-rich Pd–Rh alloys

Urszula Koss · Mariusz Łukaszewski ·
Katarzyna Hubkowska · Andrzej Czerwiński

Received: 30 March 2011 / Revised: 20 July 2011 / Accepted: 21 July 2011 / Published online: 3 August 2011
© The Author(s) 2011. This article is published with open access at Springerlink.com

Abstract Hydrogen electrosorption into Pd-rich (>80 at.% Pd in the bulk) Pd–Rh alloys has been studied in acidic solutions (0.5 M H₂SO₄) using cyclic voltammetry and chronoamperometry. The influence of temperature (in the range between 283 and 328 K), electrode potential and alloy bulk composition on hydrogen electrosorption properties of Pd–Rh alloys is presented. It has been found that the additive of Rh to Pd–Rh alloys increases the maximum hydrogen solubility (for Rh bulk content below 10 at.%), decreases the potential of absorbed hydrogen oxidation peak and decreases the potential of the $\alpha \rightarrow \beta$ phase transition. Increasing temperature decreases the potential of absorbed hydrogen oxidation peak, the maximum hydrogen solubility, and the potential of the $\alpha \rightarrow \beta$ phase transition. The amounts of electrosorbed hydrogen for α - and β -phase boundaries, i.e., α_{\max} and β_{\min} , have been determined from the integration of the initial parts of current–time responses in hydrogen absorption and desorption processes. The H/M ratio corresponding to α_{\max} increases with increasing Rh content, while for β_{\min} a maximum of H/M ratio is observed for the alloys containing ca. 95% Rh.

Keywords Pd–Rh alloys · Hydrogen absorption · Temperature · Phase transition · Limited volume electrodes

Introduction

Nowadays, when the supplies of natural resources, such as coal, natural gas, or petroleum, are almost depleted, it

seems necessary to search for new sources of energy. Thanks to its numerous advantages (such as high value of energy, availability, non-toxicity) hydrogen has become a subject of research for many scientists. However, high cost of hydrogen technologies and the danger of explosion connected with hydrogen storage in gas or liquid phase are the main barriers against its widespread application. Thus, hydrogen storage in the form of metal hydrides seems to be much more safe, economic, and convenient [1].

One of the metals able to absorb large amounts of hydrogen is palladium. Unfortunately, due to its high cost and great atomic mass palladium cannot be used in a practical way on a large scale. Nevertheless, palladium–hydrogen and palladium alloy–hydrogen systems are model systems widely studied to understand the process of hydrogen absorption in solid materials.

Pd and Rh belong to platinum group metals; however, their hydrogen sorption properties are markedly different. Under normal conditions the maximum amount of hydrogen dissolved in Pd corresponds to the hydrogen-to-metal (*H/M*) ratio of ca. 0.69 [2], which means that the volume of hydrogen gas absorbed is ca. 950 times greater than the volume of the Pd specimen itself. On the other hand, hydrogen absorption in Rh requires extremely high hydrogen pressures (of the order of GPa) [3] and under normal conditions this metal can only adsorb hydrogen on the surface.

The general rule is that Pd alloys with a non-absorbing metal (e.g., Au, Ag, and Pt) are characterized by a decrease in the maximum amount of absorbed hydrogen [2, 4]. This behavior is explained by the electronic effect. According to the band model the gaps in the Pd d-band are partially filled by the other metal's electrons and therefore less gaps remain for the electrons from absorbed hydrogen [2, 4]. However, Pd–Rh alloys are an exceptional system in that

U. Koss · M. Łukaszewski · K. Hubkowska · A. Czerwiński (✉)
Faculty of Chemistry, University of Warsaw,
Pasteura 1,
02-093 Warsaw, Poland
e-mail: aczerw@chem.uw.edu.pl

the amount of absorbed hydrogen is larger (for Pd-rich alloys) than in case of pure Pd [5–9]. In the case of low Rh content there is an increase in the number of gaps in the Pd *d*-band below Pd Fermi level [4], which is manifested by an increase in the maximum amount of hydrogen absorbed in Pd–Rh alloys. The literature gives different information about Rh bulk content in Pd–Rh alloys corresponding to the highest amount of absorbed hydrogen. Most literature data indicate that the highest ability to absorb hydrogen is exhibited by Pd–Rh alloys containing 2–10 at.% Rh in the bulk [5–9]. However, some results suggest that alloys containing even ca. 20% Rh can still absorb high amounts of hydrogen [9, 10]. Moreover, the composition range where two phases of absorbed hydrogen can coexist also seems to be greater than for other Pd alloys [9, 11]. Crystallographic data [11] indicate that the β phase can be formed at least up to 20% Rh in the bulk. Our earlier results [9] suggest that at room temperature the second phase in the Pd–Rh–H ternary system exists up to ca. 35% Rh in the bulk. According to various authors the limiting Rh content for which the ability to absorb hydrogen ceases lies in the range 20–45% Rh in the bulk [5, 6, 9].

Hydrogen absorption in Pd alloys has also been studied theoretically. Density functional (DFT) calculations of the interaction of molecular hydrogen with transition metals were studied by Bartczak [12], who compared a H_2 –AgPd system with a H_2 –Pd₂ system. In a symmetric system H_2 –Pd₂ charge displacement between protons is not observed (in contrast to H_2 –AgPd), but the strong affinity of hydrogen to palladium is manifested here by the shape of the area of high electron density for small *d* (distance between the center of the H–H bond and the center of the dimer; e.g., *d*=1 Å) distances. The area of high density form a bridge from one of the Pd atoms through the two protons to the second Pd atom. It should be noted that without the mediation of the hydrogen the area of high electron density between atoms of palladium does not exist. The overall view of the evolution of the electrons distribution in the system H_2 –Pd₂ with the approach of hydrogen to palladium also shows the dissociation of H_2 molecule, but this is the dissociation into H atoms, not into H⁺ and H[−] ions like in case of AgPd. However, these calculations have to be extended from model systems to a much larger dimer cluster systems.

Løvnik and Olsen [13] also used the DFT method to calculate equilibrium lattice constant of Pd_{4−*n*}Ag_{*n*} (*n*=0–4) with and without hydrogen and the value of absorption energy. The lattice constant of mentioned system was estimated from generalized gradient approximation, which is used for every 4*d* transition metals. Obtained results, showing 5.2% increase in the lattice constant with Ag content, were very close to the experimental data. Considering hydrogen absorption, the most stable site of each

hydride was pointed from the relation of calculated absorption energy and hydrogen content, (e.g., Pd₃Ag has the most stable hydrogen absorption site at 25% of hydrogen content). This relation allows also to find that the solubility of hydrogen in the alloys decreases with increasing Ag content, what is called as an electronic effect.

Recently, we have published numerous papers on the electrochemistry of Pd alloys, including Pd–Rh alloys [9, 14–19]. The processes of hydrogen electrosorption, surface oxidation, and metal dissolution as well as adsorption of carbon oxides were examined. However, all these experiments were performed at room temperature only. In this report, we present the results of the investigations on hydrogen absorption properties of Pd–Rh alloys at different temperatures (in the range 283–328 K). With this work we continue our earlier studies on the influence of temperature on hydrogen electrosorption into Pd alloys with other metals prepared as thin electrodeposits (limited volume electrodes) [20–22]. We demonstrate here the influence of deposition potential and bath compositions on alloy bulk composition and the influence of temperature and Rh bulk content on the amount of absorbed hydrogen, the potential of absorbed hydrogen oxidation, and the potential of the $\alpha \rightarrow \beta$ phase transition. We compare the results obtained for Pd–Rh alloys with our previous data for Pd–Au and Pd–Pt alloys [20–22].

Experimental

All experiments were performed in 0.5 M H_2SO_4 solutions at temperature of 283, 298, 313, and 328 K, controlled by a thermostat (Lauda RE 306, Germany). The solutions were prepared from analytical grade reagents and triply distilled water additionally purified in a Millipore system. Before the experiments the electrolyte was deoxygenated with an argon (99.999%) stream for 15 min; during the experiments the argon stream was directed above the solution level in order to avoid contact with air. A Hg|Hg₂SO₄|0.5 M H_2SO_4 was used as the reference electrode. A Pt gauze was used as the auxiliary electrode.

The reference electrode and Pt gauze were maintained in the same temperature as the rest of the electrochemical cell. The temperature dependence of the reference electrode potential in the range of 283–328 K was determined through open circuit potential measurements in a cell consisting of the reference electrode and a saturated calomel electrode, using Multifunction Computer Meter (Elmetron Company). The potentials of the reference electrode versus SHE at various temperatures were calculated using the values of potentials of calomel electrode drawn from the chemical tables [23].

With the exception of Fig. 1, all potentials were recalculated with respect to the RHE on the basis of the literature data [24], according to which the potential of $\alpha \rightarrow \beta$ phase

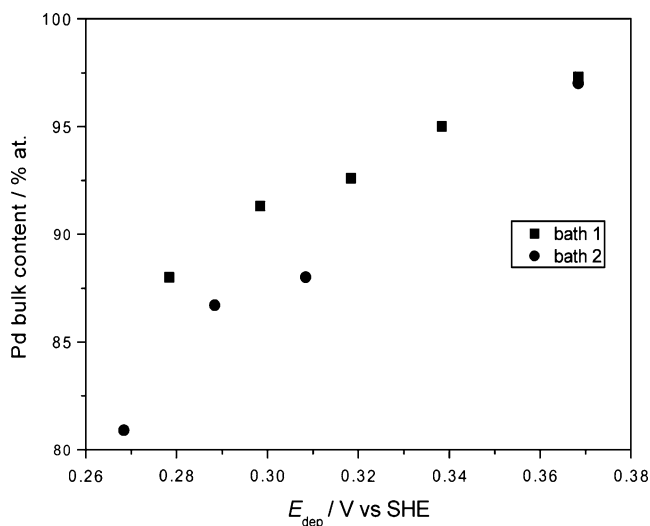


Fig. 1 The influence of deposition potential on Pd bulk concentration in Pd–Rh alloys (298 K). Bath compositions: bath 1–0.06 M RhCl_3 +0.10 M PdCl_2 +0.89 M HCl, bath 2–0.10 M RhCl_3 +0.09 M PdCl_2 +0.80 M HCl. Note: the potential scale is vs. SHE, not RHE (as in other figures)

transition for hydrogen-saturated palladium electrode at 298 K is 50 mV vs. RHE. Taking into account that in our measurements the $\alpha \rightarrow \beta$ phase transition potential at 298 K was 22 mV vs. SHE, it was possible to calculate the activity of H^+ ions in 0.5 M H_2SO_4 aqueous solution and then to recalculate the potentials at given temperature, using the equation:

$$E_{\text{vs.RHE}} = E_{\text{vs.SHE}} - (RT/F)\ln a_{\text{H}^+}$$

It should be added that a very similar value of H^+ ion activity was obtained from the calculations based on the extended Debye–Hückle law.

The working electrode was a gold wire (99.99%, 0.5 mm diameter) covered with a thin alloy layer electrodeposited at a constant potential from a bath containing aqueous solutions of PdCl_2 and RhCl_3 with the addition of HCl. Various alloy compositions were obtained by changing bath composition and deposition potential [9, 17]. After electrochemical measurements the electrodes were dissolved in aqua regia and the total amounts of Pd and Rh in the alloys were analyzed by atomic emission spectroscopy. The efficiency of electrodeposition was in the range of 93–100%. The alloy thickness was ca. $1.0 \pm 0.1 \mu\text{m}$. All alloy compositions are bulk compositions expressed in atomic percentages.

At the beginning of hydrogen absorption experiments each electrode was subjected to a series of voltammetric and chronoamperometric scans/steps through the potential region of hydrogen adsorption and absorption until a steady-state voltammogram was obtained. This procedure was applied in order to avoid the effects of aging during

further hydrogen insertion/removal [20, 21, 25, 26]. Hydrogen absorption was performed at a constant potential for a period sufficient to ensure full hydrogen saturation, determined by chronoamperometry. Hydrogen was desorbed voltammetrically with scan rate of 0.01 V s^{-1} . It was demonstrated in earlier studies [14] that under these conditions all absorbed hydrogen can be removed from the electrode in an electrochemical process, which means that the total amount of absorbed hydrogen can be determined from the charge due to its oxidation.

Results and discussion

Influence of deposition potential on Pd bulk content in Pd–Rh alloys

Figure 1 shows the influence of deposition potential on Pd bulk concentration in Pd–Rh alloys. The temperature of deposition was 298 K. Baths used for deposition were composed of aqueous solutions of PdCl_2 , RhCl_3 , and HCl. Bath 1 contained 0.06 M RhCl_3 , 0.10 M PdCl_2 , and 0.89 M HCl, while bath 2 contained 0.10 M RhCl_3 , 0.09 M, PdCl_2 and 0.80 M HCl.

For both baths decreasing deposition potential resulted in lower Pd bulk content. In the case of bath 2 a slight change in deposition potential (by 0.05 V) caused a greater difference in Pd bulk concentration (by ca. 10 at.%) than a similar alteration of deposition potential for the bath 1 (by ca. 5 at.%). These trends were in line with the results reported in our earlier paper [17], where the electrochemical preparation and characterization of thin deposits of Pd–Rh and other Pd-noble metal alloys have been described in detail. The increase in bulk Pd content in alloys with the increase in deposition potential from chloride solutions was observed also for Pd–Pt alloys, while for Pd–Au alloys an opposite effect occurred [20, 22].

Figure 1 demonstrates that using the above two deposition baths and deposition potentials in the range 0.27–0.37 V vs. SHE it was possible to obtain Pd–Rh alloys with Pd bulk concentration ranging from ca. 81 to 98 at.%. It should be added that the deposition potential was always higher than the value required for hydrogen sorption in order to eliminate a simultaneous hydrogen penetration into the deposited alloy.

Influence of electrode potential on chronoamperometric signals of hydrogen absorption and desorption

Figure 2 shows the examples of chronoamperograms recorded during hydrogen absorption and desorption at various potentials and temperatures for a Pd–Rh alloy (92.6% Pd in the bulk). In the cathodic potential step a

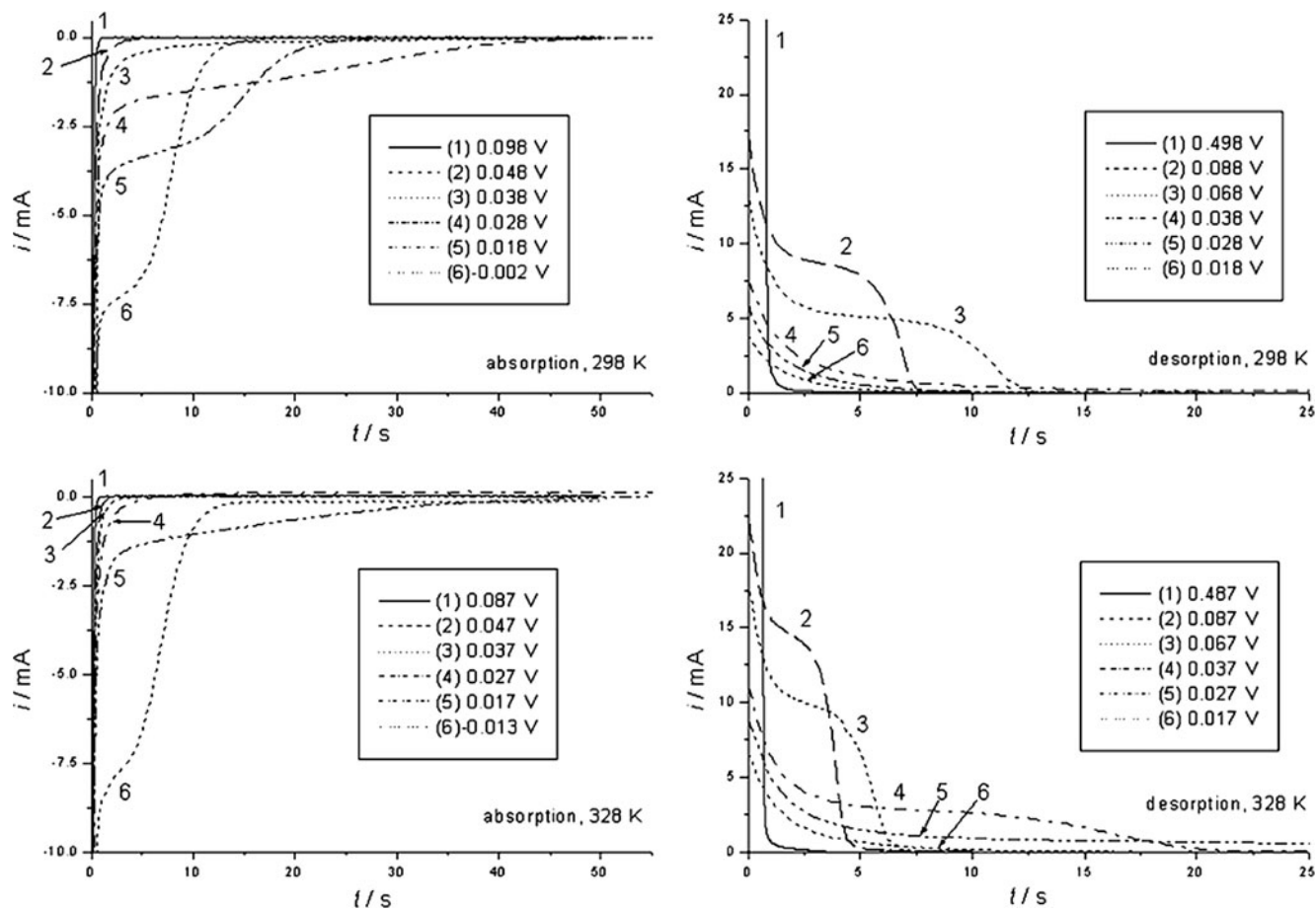


Fig. 2 Chronoamperograms recorded during hydrogen absorption (potential steps from 0.50 V to different values indicated in the legend) and during hydrogen desorption (potential steps from -0.01 V to different

values indicated in the legend) for a Pd–Rh alloy (92.6% Pd in the bulk) at temperatures of 298 and 328 K

current is flowing due to the reduction of H^+ ions to H atoms adsorbed on the surface, which further undergo insertion into metal lattice, where a particular phase of absorbed hydrogen is formed [27] (alternatively, according to a model of a direct absorption [28–31], H^+ ions are reduced and hydrogen is incorporated into metal in a single step, i.e., without the adsorbed intermediate). For relatively high potentials (above ca. 0.03 V) the reduction current is small and rapidly drops to zero when the electrode becomes saturated with absorbed hydrogen. As can be deduced from the charges due to hydrogen absorption, at those potentials only the α phase of absorbed hydrogen (i.e., a solid solution of hydrogen in metal) can exist (see Fig. 5 below). The time needed for a complete electrode saturation with hydrogen becomes longer with decreasing absorption potential, i.e., when the amount of absorbed hydrogen increases (Fig. 3). The longest absorption time is observed for the potential, where the hydrogen-rich β phase (i.e., a non-stoichiometric metal hydride) can be formed. With a further potential decrease the absorption time decreases despite the still increasing amount of absorbed hydrogen.

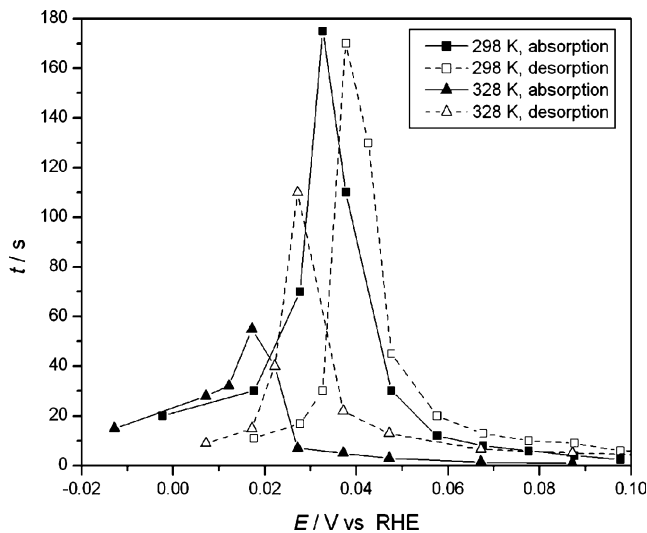


Fig. 3 Influence of electrode potential on time needed for hydrogen absorption (potential steps from 0.50 V to different values indicated on the x-axis) and desorption (potential steps from -0.01 V to different values indicated on the x-axis) for a Pd–Rh alloy (92.6% Pd in the bulk) at temperatures of 298 and 328 K. Solid symbols, solid lines—absorption course, open symbols, dashed lines—desorption course

Simultaneously, for the potentials corresponding to the β -phase formation a characteristic inflection point appears on the initial part of CA curves, where after a rapid current drop the slope of the $i-t$ curve is reduced. Earlier studies [20–22] on Pd–Au and Pd–Pt alloys indicated that this point corresponds to the onset of the $\alpha \rightarrow \beta$ phase transition. For sufficiently low potentials hydrogen absorption is accompanied by hydrogen evolution and after the complete electrode saturation with absorbed hydrogen a residual current due to hydrogen evolution is flowing.

Qualitatively similar tendencies are observed in the course of anodic CA curves for increasing potential of desorption of hydrogen previously absorbed in the β phase. At low desorption potentials (below 0.03 V) the β phase cannot be totally decomposed, which results in a small anodic current decaying in a short time. Hydrogen oxidation current and desorption time increase with increasing desorption potential. The longest time needed for hydrogen oxidation is observed for a potential where the $\beta \rightarrow \alpha$ phase transition occurs and with a further increase in desorption potential the time becomes shorter (see Fig. 3). Again, an inflection point appears on CA curves indicating the onset of the $\beta \rightarrow \alpha$ phase transition. As demonstrated in our earlier papers [9, 22, 32], these trends are a consequence of the fact that for thin Pd-based layers in the presence of both phases of absorbed hydrogen the rates of the processes of hydrogen absorption and desorption are controlled by the rates of the $\alpha \rightarrow \beta$ and $\beta \rightarrow \alpha$ phase transitions, respectively. The influence of the rate of the phase transition on hydrogen electro sorption currents was also demonstrated by theoretical modeling of CV responses for thin Pd layers [33].

Influence of electrode potential on voltammetric signals of hydrogen desorption

Figure 4 shows anodic voltammetric signals (0.01 Vs^{-1}) due to the oxidation of hydrogen electro sorbed at various potentials. Data for a Pd–Rh alloy (92.6 at.% Pd) at four different temperatures (283, 298, 313, and 328 K) are presented in the left column, while in the right column the curves for Pd and three alloys of different bulk compositions (95.0, 88.0, and 80.9 at.% Pd) at 298 K are shown.

On each graph in Fig. 4 two regions of hydrogen oxidation can be distinguished. At low values of the potentials, a well-defined anodic peak (I) is present, while at higher potentials a small oxidation current (II) appears. These two potential regions of hydrogen oxidation correspond to different forms of absorbed hydrogen. The peak at lower potentials originates from the oxidation of hydrogen absorbed mainly in the β phase as well as small amounts of adsorbed hydrogen (and low quantity of adsorbed hydrogen in the α phase) [9, 14, 34]. The signal at higher potential

corresponds to the oxidation of mainly adsorbed hydrogen and absorbed in the α phase [9, 14, 34]. It is worth noting that the electro sorption potential has little influence on the signals in region (II), but has a very large impact on the size and shape of the peak (I), i.e., in the region where the hydrogen-rich β phase exists. It was confirmed [14] that signal (II) shows a greater electrochemical reversibility than signal (I). The reason is that the significant contribution to the former signal originates from a surface process, i.e., it is hydrogen adsorption/desorption, which is much faster than the absorption process [14, 22].

Figure 4 confirms a well-known fact that the height and charge under the hydrogen desorption signals increase with decreasing saturation potential [6, 14, 19–22]. Therefore, the amount of adsorbed hydrogen strongly depends on the electro sorption potential. It can be seen that the most dramatic increase in the height and charge under this peak (i.e., the amount of adsorbed hydrogen) is observed when the potential value approaches the potential of the $\alpha \rightarrow \beta$ phase transition. This conclusion is consistent with the studies based on the hydrogen saturation of palladium and alloys from the gas phase, where the higher pressure corresponds to a lower potential [2]. It is worth noting that the potential impact on the shape and size of the peak (I) varies with the alloy bulk composition. For palladium and Pd-rich alloys (100 at.% Pd, 95.0 at.% Pd) the effect is stronger than for alloys containing more rhodium (88.0 at.% Pd, 80.9 at.% Pd). The evolution of CV curves with electro sorption potential for hydrogen oxidation on Pd and its alloys was discussed earlier [9, 14, 22, 34].

Figure 4 also shows that the alloy composition affects the potential of the hydrogen oxidation peak (I), i.e., the higher the Rh bulk content in the alloy, the lower the peak potential. The negative shift in the peak potential between pure Pd and a Pd–Rh alloy containing 80.9% Pd reaches ca. 80 mV at 298 K. This behavior indicates that the additive of Rh facilitates the kinetics of the oxidation of adsorbed hydrogen. Palladium alloys with gold and platinum exhibited the same tendency [19–22]. These effects were discussed in detail in our recent paper [18]. It was suggested that Pd alloying with other metals could facilitate the process of hydrogen electro sorption, with the influence on the rate of the phase transition as one of the key factors [18].

The comparison of dependencies registered at different temperatures confirms the previously established conclusion that the hydrogen oxidation peaks are shifted towards lower values of the potentials with increasing temperature [19–22, 34]. In addition, it can be noted that the height of the hydrogen desorption signal slightly increases with temperature and its width decreases. This behavior is a consequence of the facilitated kinetics of hydrogen absorption/desorption at elevated temperature [18–22, 35].

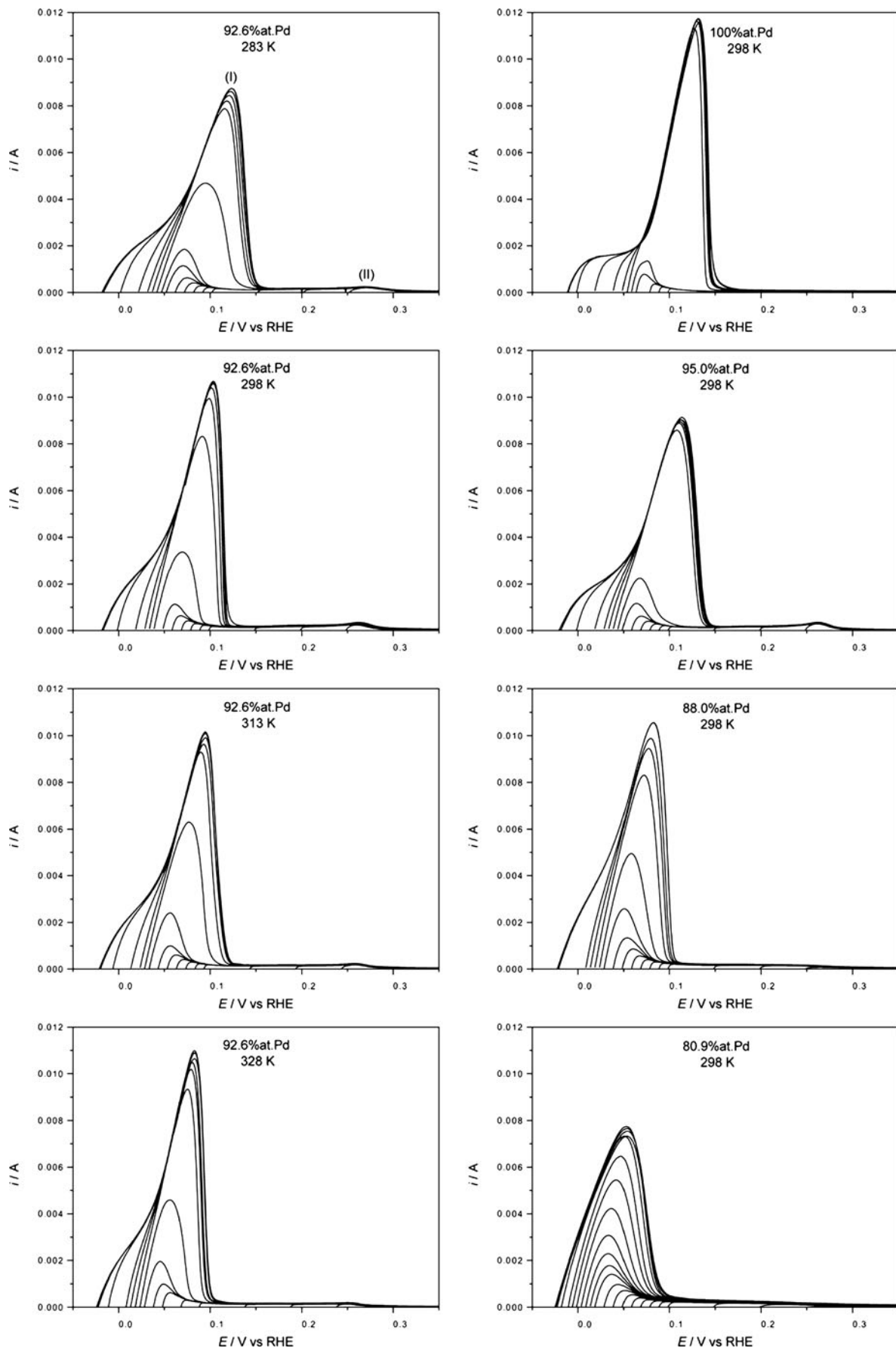


Fig. 4 Anodic voltammetric scans (0.01 V s^{-1}) recorded in $0.5 \text{ M H}_2\text{SO}_4$ after hydrogen electro sorption at various potentials for a Pd–Rh alloy with 92.6 at.% Pd at four temperatures: 283 K, 298 K, 313 K, and 328 K (*left column*) and for Pd and three Pd–Rh alloys of different bulk compositions (95.0, 88.0, and 80.9 at.% Pd) at temperature of 298 K (*right column*)

Influence of electrode potential, alloy bulk composition, and temperature on hydrogen absorption capacity of Pd–Rh alloys

Figure 5 shows the influence of electrode potential on the amount of electro sorbed hydrogen (presented as a hydrogen-to-metal atomic ratio, H/M) in Pd and Pd–Rh alloy of various bulk compositions, at different temperatures. The amount of absorbed hydrogen was calculated from hydrogen oxidation charges obtained by the integration of cyclic voltammetric curves recorded during hydrogen desorption.

The specific shape of the obtained curves corresponds to different forms of hydrogen absorbed in alloy. With decreasing potential, initially a plateau is observed in the region of the presence of the α phase. Then one can notice a sudden increase in H/M ratio in a narrow range of potentials, which is described as a $\alpha \rightarrow \beta$ phase transition, followed by another plateau in the presence of the β phase.

The contribution from adsorbed hydrogen can be estimated on the basis of electrode thickness and surface roughness. The electrodes were ca. $1 \mu\text{m}$ thick, which corresponds to more than 5,000 atomic layers with the roughness factor in the range 100–300. Thus, in the presence of a monolayer of adsorbed hydrogen the contribution from hydrogen adsorption is only a small fraction of the total amount electro sorbed hydrogen. Our estimations made for Pd-rich Pd–Rh alloys [16] showed that for the α phase the value of surface coverage with adsorbed hydrogen is only ca. 0.10, while for the saturated

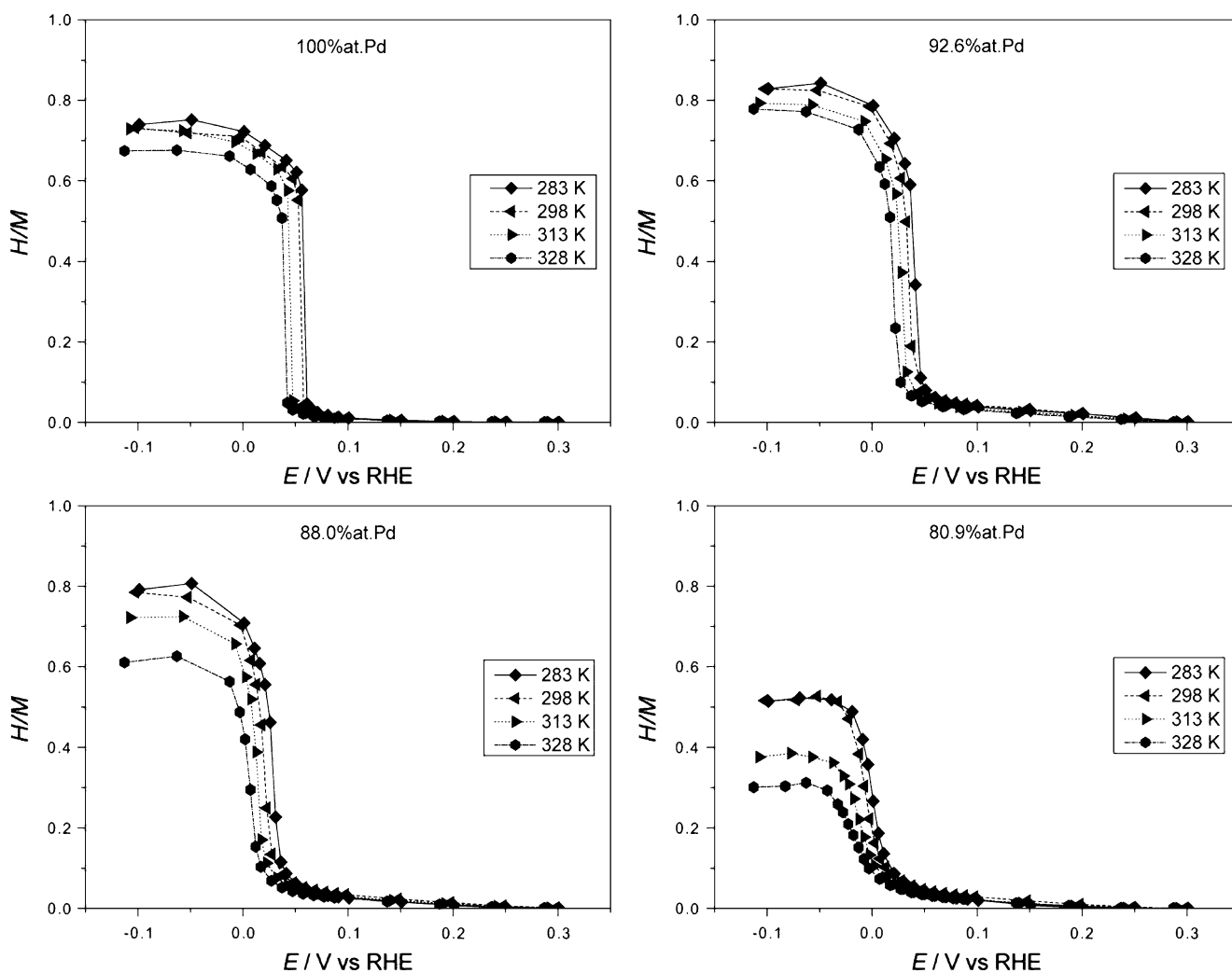


Fig. 5 The amount of absorbed hydrogen (expressed as hydrogen-to-metal atomic ratio) from $0.5 \text{ M H}_2\text{SO}_4$ vs. electrode potential obtained at various temperatures (283 K, 298 K, 313 K, and 328 K) for Pd and three Pd–Rh alloys with 92.6, 88.0, and 80.9 at.% Pd

β phase it reaches ca. 0.60. Taking into account the H/M ratios for both phases, namely ca. 0.10 for the maximum saturation in the α phase and ca. 0.80 for the maximum saturation in the β phase, it is clear that for the electrode thickness of 1 μm (i.e., ca 5,000 atomic layers) and the roughness factor of 300, for the H/M ratio within the entire sample the effect of adsorbed hydrogen is smaller than 1.5%.

In regard to other types of alloys, e.g., Pd–Au [20, 36–38] or Pd–Pt [21, 34, 39–41], the Pd–Rh system demonstrates a very unusual hydrogen absorption behavior. With the addition of a small amount of Rh the maximum alloy absorption capacity in the β phase increases [4–9]. We have found that in the temperature range of 283–328 K the alloy which absorbs the largest amount of hydrogen consists of 92.6% of Pd in the bulk. This is in line with our earlier study [9], where the maximum ability to absorb hydrogen was exhibited by an alloy with ca. 94 at.% Pd.

Simultaneously, Pd alloying with Rh causes that hydrogen absorption curves are shifted negatively at the potential scale. The potential of the $\alpha \rightarrow \beta$ phase transition for Pd–Rh alloys is lower than for pure Pd, which means that under gas phase conditions the corresponding hydrogen pressure is higher. The shift of the potential (pressure) corresponding to the phase transition is explained by the geometric effect, i.e., changes in the dimensions of the unit cell after alloy formation [11, 42–45]. In general, for most of the Pd alloys of a lattice constant higher than that of pure Pd (expanded systems) an increase in potential (decrease in pressure) is observed for the phase transition due to the fact that the work needed to increase the dimensions of the crystal lattice during the β phase formation is smaller. On the other hand, in the case of alloys with a lattice constant lower than pure Pd (contracted systems) there is a need for an additional work connected with the increasing size of the crystal lattice during hydrogen absorption in the β phase, which is mirrored in a decrease in potential (increase in pressure) for the phase transition. Pd–Rh alloys belong to the second group of systems [11]. However, more recent DFT calculations suggest that the influence of the electronic structure is even more important than the effect of the lattice constant to explain the variation in absorbed hydrogen stability in Pd alloys [46].

It should be stressed that hydrogen absorption experiments revealed bulk homogeneity of our Pd–Rh electrodes. This conclusion can be drawn from the fact that only one α – β phase transition region was observed, whose potential changed with the alloy bulk composition. We did not observe more phase transition regions, a feature characteristic of alloys exhibiting phase separation. As we demonstrated in our earlier paper [15], the potential of the α – β phase transition for electrodeposited Pd–Pt, Pd–Rh, Pd–Pt–Rh, and Pd–Au alloys correlated with the alloy bulk

composition, indicating that the hydrogen absorbing phase was the only phase present in the system. The formation of a homogeneous solid solution during codeposition of Pd with Pt and Rh was confirmed by XRD analysis in another work [32].

Temperature also has a significant influence on absorption capacities and potential of the $\alpha \rightarrow \beta$ phase transition (Fig. 5). With increasing temperature the maximum amount of electroadsorbed hydrogen becomes lower, which is consistent with the fact that hydrogen absorption in Pd-rich alloys is an exothermic process [2, 20, 21, 36, 37, 39]. The potential of the $\alpha \rightarrow \beta$ phase transition is shifted towards negative values with increasing temperature, which corresponds to the increase in hydrogen pressure during absorption from the gas phase [2].

Wicke and Brodowski studied hydrogen in palladium and its alloys from the gas phase [47]. Isotherms of hydrogen absorption in palladium at different temperatures are composed of three distinct parts: the first one (the growing) refers to the α phase, the second one (at constant pressure)—the two phase region $\alpha + \beta$, and the third one (again increasing)— β phase. The same relation we obtained in our electrochemical studies, where the higher potential corresponds to a lower pressure. The temperature dependence is also similar. The middle sections of horizontal isotherms narrow with increasing temperature and disappear at about 570 K (the critical temperature). Critical pressure is about 20 atm. At lower temperatures the amount of hydrogen absorbed in the form of α phase is smaller than the corresponding amount absorbed during this phase at higher temperatures.

It should be noted that temperature has greater effect on the absorption capacity for the alloys with a lower Pd content. For instance, for an alloy containing 88.0% Pd in the bulk the maximum amount of hydrogen absorbed at room temperature (298 K) is higher than for pure Pd, while for the same alloy at 328 K the maximum absorption capacity is lower than that of Pd. On the other hand, for the alloy containing 92.6% Pd its absorption capacity is greater as compared to Pd at all temperatures studied.

Figure 6 shows the influence of alloy bulk composition on the amount of hydrogen electroadsorbed at various potentials. It is evident that the amount of electroadsorbed hydrogen depends on the bulk composition of Pd–Rh alloys and the exact course of this dependence also varies with the value of the applied potential.

It can be noticed that at high potentials the amount of electroadsorbed hydrogen is small and almost independent of Pd content in the alloy bulk. For an experiment carried out in 298 K the amount of absorbed hydrogen starts to increase with Pd concentration from the potential of ca 0.053 V and a rapid jump of H/M ratio can be seen between alloys including 97.3% and 100% Pd in bulk. With

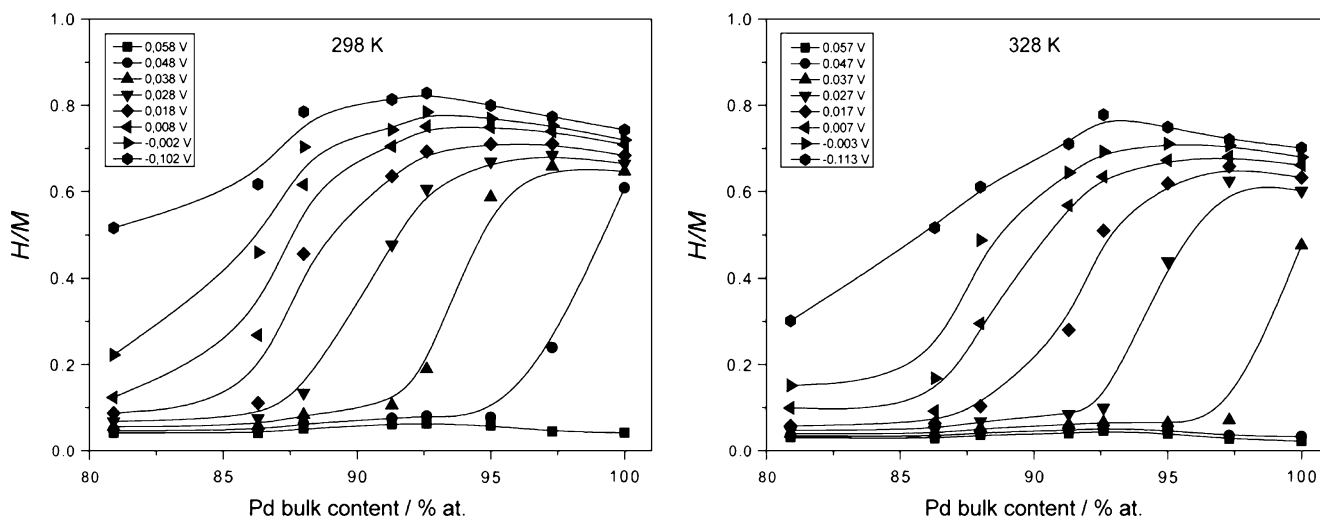


Fig. 6 The influence of alloy bulk composition on the amount of hydrogen absorbed from 0.5 M H₂SO₄ at various potentials in Pd–Rh alloys at temperatures of 298 K and 328 K

decreasing potential the “jump point” shifts towards alloys containing less Pd and, additionally, when potential reaches a value of about 0.028 V for small Rh contents a maximum appears on the dependence of H/M ratio on alloy bulk composition. This maximum shifts towards higher Rh bulk concentration with a potential decline. These trends can be explained taking into account geometric and electronic effects. In the case of relatively high potential values geometric effect dominates, which is reflected as a decrease in the amount of electroadsorbed hydrogen with increasing Rh bulk content.

Interestingly, the same behavior is observed for Pd–Pt alloys [22]. However, in the case of Pd–Rh alloys for sufficiently low potential values the electronic effect starts to be prevalent and this can be noticed as a maximum of H/M value (e.g., at 283 K for –0.102 V first the amount of electroadsorbed hydrogen increases with Rh bulk content, attains maximum for alloy containing 92.6% and then decreases). In regard to the presence of the aforementioned maximum Pd–Rh alloys exhibit a similar behavior to Pd–Au alloys [14, 22]. However, in the latter case the maximum was observed only at higher potential region and was due to the positive geometric effect, while at lower potentials the electronic effect caused a decrease in hydrogen solubility in Pd–Au alloys. Thus, depending on different values of potentials and electrode bulk composition, the observed hydrogen absorption behavior is a result of a dominance of either electronic or geometric effect, together with the influence of some other factors, such as changes in elastic properties (e.g., for Pd–Pt alloys [48]).

In various temperatures the relations described are similar and differ only in the values of the characteristic potentials. Again, the general trend is observed to a decrease in H/M values with increasing temperature.

However, the composition of the alloy with a maximum ability to absorb hydrogen (92.6% Pd) remains constant in the temperature range studied. With a further Pd substitution with Rh the alloy ability to absorb hydrogen decreases, although at lower temperatures for alloys containing more than ca. 85% Pd in the bulk it is still relatively high. The maximum amount of adsorbed hydrogen decreases with increasing temperature, especially for alloys containing less than 90% Pd. This effect is well pronounced for the alloys containing 80.9% Pd in the bulk, where at 298 K the maximum absorption capacity corresponds to H/M ratio of almost 0.55, while at 328 K it reaches only 0.30.

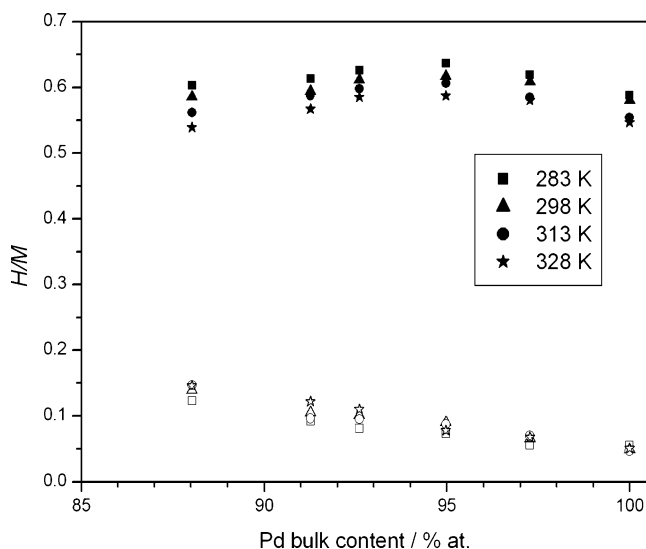


Fig. 7 Influence of temperature and alloy bulk composition on the amount of electroadsorbed hydrogen (expressed as hydrogen-to-metal atomic ratio) for the α - (open symbols) and β -phase (solid symbols) boundaries

These results are in line with other authors' reports on hydrogen absorption in Pd–Rh alloys both under gas phase and electrochemical conditions [5–9]. Thus, the absorption properties of Pd–Rh alloys are an exception to a general rule that Pd alloying with a non-absorbing element causes a deterioration of the hydrogen absorption capacity [2]. This unusual behavior of Pd-rich Pd–Rh alloys is explained by the electronic effect, i.e., the increase in the number of holes in Pd d-band after the addition of small amounts of Rh [4].

Since in CA curves shown in Fig. 2 the characteristic inflection points indicate the onset of the phase transitions [22, 32], by the integration of the initial parts of chronoamperograms it is possible to determine the limiting hydrogen concentrations corresponding to maximum saturation in the α phase (α_{\max}) and the minimum saturation in the β phase (β_{\min}). Figure 7 shows the amounts of hydrogen for the phase boundaries as a function of alloy bulk composition and temperature. It is demonstrated that the values of hydrogen concentration for α_{\max} increase with increasing amount of Rh in the alloy bulk, being rather weakly dependent on temperature in the range 283–328 K. On the other hand, the values for β_{\min} initially increase with increasing Rh content reaching a maximum for ca. 5% Rh, followed by a slow decrease for alloys containing more Rh. The minimum amount of hydrogen absorbed in the β phase decreases with increasing temperature leading to a slight decrease in the miscibility gap in the alloy–hydrogen system. Due to the fact that with the greater additive of Rh to Pd the inflection points on CA curves became less pronounced, it was difficult to determine hydrogen concentrations at the phase boundaries for Pd–Rh alloys containing less than ca. 88% Pd in the bulk. However, for this composition the two limiting concentrations of hydrogen are markedly different (i.e., $\beta_{\min} \neq \alpha_{\max}$), which indicates that two separate phases of absorbed hydrogen still exist in those alloys. A rough extrapolation of the curves for both phase boundaries suggests that the two-phase region in the Pd–Rh–H system disappears at ca. 75% Rh. This value is by ca. 10% higher than that estimated on the basis of the shape of H/M vs. potential curves, reported in our earlier study [9]. However, the tendencies shown in Fig. 7 are qualitatively similar to the trends in the limiting values of lattice parameters for the α - and β -phase boundaries reported earlier in the literature [11], where it is demonstrated that for Pd–Rh alloys containing at least 20% Rh the β phase of absorbed hydrogen can be formed.

Conclusions

The addition of small amounts of Rh (below 10 at.%) to Pd–Rh alloys increases the maximum hydrogen solubility in the β

phase region. In the temperature range between 283 and 328 K the maximum H/M ratio, exceeding 0.80, is exhibited by a Pd–Rh alloy containing 92.6% Pd in the bulk. Further decrease in the amount of Pd in the alloy bulk leads to a deterioration of the ability to absorb hydrogen, although at low temperatures (283 K) the absorption capacity of Pd–Rh alloys containing more than 80% Pd is still comparable with that of pure Pd. Pd alloying with Rh results also in a negative shift of both the potential of absorbed hydrogen oxidation peak and the potential of the $\alpha \rightarrow \beta$ phase transition, which means that the β phase is kinetically and thermodynamically less stable than in pure Pd.

Increasing temperature results in the following trends in hydrogen electrosorption properties of Pd and Pd–Rh alloys: (1) a decrease in the potential of absorbed hydrogen oxidation peak, (2) a decrease in the maximum hydrogen solubility, and (3) a decrease in the potential of the $\alpha \rightarrow \beta$ phase transition. Thus, temperature increase facilitates the kinetics of hydrogen oxidation but also weakens the alloy absorption capacity and makes the formation of the β phase thermodynamically less favorable.

Open Access This article is distributed under the terms of the Creative Commons Attribution Noncommercial License which permits any noncommercial use, distribution, and reproduction in any medium, provided the original author(s) and source are credited.

References

- Crabtree GW, Dresselhaus S, Buchanan MV (2004) *Physics Today* 57:39
- Lewis FA (1967) *The palladium–hydrogen system*. Academic, London
- Tkacz M (1998) *J Chem Phys* 108:2084
- Wicke E, Frölich K (1989) *Z Phys Chem NF* 163:35
- Barton JC, Green JAS, Lewis FA (1966) *Trans Faraday Soc* 62:960
- Lewis FA, McFall WD, Witherspoon TC (1973) *Z Physik Chem NF* 84:31
- Sakamoto Y, Haraguchi Y, Ura M, Chen FL (1994) *Ber Bunsenges Phys Chem* 98:964
- Sakamoto Y, Ishimaru N, Hasebe M (1994) *Z Phys Chem* 183:319
- Żurowski A, Łukaszewski M, Czerwiński A (2006) *Electrochim Acta* 51:3112
- Comisso N, De Ninno A, Del Giudice E, Mengoli G, Soldan P (2004) *Electrochim Acta* 49:1379
- Sakamoto Y, Baba K, Flanagan TB (1988) *Z Phys Chem NF* 158:223
- Bartczak W, Romanowski S, Łandwilt M (2001) *Wiad Chem* 55:629
- Løvvik OM, Olsen R (2002) *J Alloy Comp* 330–332:332
- Łukaszewski M, Grdeń M, Czerwiński A (2006) *J New Mat Elect Syst* 9:409
- Łukaszewski M, Żurowski A, Grdeń M, Czerwiński A (2007) *Electrochem Commun* 9:671
- Żurowski A, Łukaszewski M, Czerwiński A (2008) *Electrochim Acta* 53:7812
- Łukaszewski M, Czerwiński A (2010) *Thin Solid Films* 518:3680

18. Łukaszewski M, Klimek K, Żurowski A, Kędra T, Czerwiński A (2011) *Solid State Ionics* 190:18
19. Łukaszewski M, Hubkowska K, Czerwiński A (2010) *Phys Chem Chem Phys* 12:14567
20. Hubkowska K, Łukaszewski M, Czerwiński A (2010) *Electrochim Acta* 56:235
21. Hubkowska K, Łukaszewski M, Czerwiński A (2011) *Electrochim Acta* 56:2344
22. Łukaszewski M, Hubkowska K, Czerwiński A (2011) *J Electroanal Chem* 651:131
23. Mizerski W (2003) *Chemical tables* (in Polish). Adamantan, Warsaw
24. Flanagan TB, Lewis F (1959) *Trans Faraday Soc* 55:1409
25. Łukaszewski M, Kędra T, Czerwiński A (2010) *Electrochim Acta* 55:1150
26. Millet P, Srour M, Faure R, Durand R (2001) *Electrochem Commun* 3:478
27. Jerkiewicz G (1998) *Prog Surf Sci* 57:137
28. Birry L, Lasia A (2006) *Electrochim Acta* 51:3356
29. Duncan H, Lasia A (2007) *Electrochim Acta* 52:6195
30. Bartlett PN, Marwan J (2004) *Phys Chem Chem Phys* 6:2895
31. Lasia A (2006) *J Electroanal Chem* 593:159
32. Łukaszewski M, Grdeń M, Czerwiński A (2004) *J Electroanal Chem* 573:87
33. Zhang W-S, Zhang X-W, Zhao X-G (1998) *J Electroanal Chem* 458:107
34. Grdeń M, Piaścik A, Koczorowski Z, Czerwiński A (2002) *J Electroanal Chem* 532:35
35. Czerwiński A, Kiersztyn I, Grdeń M (2003) *J Solid State Electrochem* 7:321
36. Maeland A, Flanagan TB (1964) *J Phys Chem* 71:1950
37. Maeland A, Flanagan TB (1965) *J Phys Chem* 69:3575
38. Łukaszewski M, Kuśmierczyk K, Kotowski J, Siwek H, Czerwiński A (2003) *J Solid State Electrochem* 7:69
39. Maeland A, Flanagan TB (1964) *J Phys Chem* 68:1419
40. Yasumatsu T, Wan JL, Matsuyama M, Watanabe K (1999) *J Alloys Comp* 900:293
41. Moysan I, Paul-Boncour V, Thiébaud S, Sciora E, Fournier JM, Cortes R, Bourgeois S, Percheron-Guégan A (2001) *J Alloys Comp* 332:14
42. Burch R (1970) *Trans Faraday Soc* 66:736
43. Flanagan TB, Sakamoto Y (1993) *Plat Met Rev* 37:26
44. Sakamoto Y, Chen FL, Ura M, Flanagan TB (1995) *Ber Bunsenges Phys Chem* 99:807
45. Sakamoto Y, Yuwasa K, Hirayama K (1982) *J Less-Common Met* 88:115
46. Ke X, Kramer GJ, Løvvik OM (2004) *J Phys Condens Matter* 16:6267
47. Wicke E, Brodowsky H (1978) Hydrogen in palladium and palladium alloys. In: Alefeld G, Völkl J (eds) *Topics in applied physics*, vol. Springer, Berlin, pp 28–29
48. Noh H, Flanagan TB, Sonoda T, Sakamoto Y (1995) *J Alloys Comp* 228:164